Experimental obviousness of the necessity for a thin Ni interfacial layer to obtain highly ordered photoconductive MoS_2 films

H. HADOUDA
L.P.M.C.E., Université d'Oran ès Sénia, BP 1642, Oran, Algeria

J. C. BERNEDE, E. GOURMELON, J. POUZET
GPSE, Equipe Couches Minces et Matériaux Nouveaux, F.S.T.N, 2 rue de la Houssinière, BP 92 208 44322 Nantes Cédex 03, France

It is shown that photosensitive films can be obtained by solid state reaction, induced by annealing, between the constituents Mo and S sequentially deposited in thin film form if the substrate is coated with a thin (10–20 nm) NiCr layer. The thin Mo and S layers are deposited in the atomic ratio Mo:S = 1:3. The substrates used are mica sheets. An annealing at 1073 K for 30 min under argon flow allows one to obtain highly 2H–MoS_2 crystallized films. The thickness of the crystallites is similar to that of the films; they have their *c*-axes perpendicular to the plane of the substrate. After crystallization, X-ray photoelectron spectroscopy (XPS) depth profiles show that Ni is diffused all over the thicknesses of the films and that 1 at% of Ni is visible at the surfaces of the films. The direct current (d.c.) conductivity of these films is nearly similar to that of single crystals. The films are photosensitive. The room temperature photoconductivity, which results from interband transitions, allows one to measure the direct band gap that is similar to that of a single crystal. When bare mica substrates (without Ni) are used MoS_2 films are obtained but they are poorly crystallized and not photoconductive, which shows an NiCr interfacial layer is necessary. Probably a melting phase NiS_x forms, which increases the mobility of the atom at grain boundaries.

1. Introduction

Transition metal dichalcogenides, MX_2 ($MoSe_2$, MoS_2, WSe_2, WS_2), are semiconductors that can act as efficient photoactive materials in the realization of photoelectrochemical [1–3] or solid device solar cells [4, 5].

For economic reasons, obtaining MX_2 in thin films would be interesting while, for ecological reasons, sulphides would be more interesting. However, if stoichiometric thin films, crystallized in the 2H–MoS_2 structure, can be easily obtained [6, 7] the films are poorly crystallized and are not photoactive.

Ennaoui *et al.* [8] have shown that it is possible to obtain textured photoconductive WS_2 films, by annealing under an H_2S atmosphere WO_3 films deposited on Ni coated substrates. However, the use of an H_2S atmosphere is quite restricting to obtain ohmic back contact. Recently Ballif *et al.* [9] have shown that textured photosensitive films can be obtained by annealing under an argon atmosphere WS_{3+x} amorphous films sputtered on an Ni coated substrate.

In this paper we use the technique of solid state reaction between the constituents sequentially deposited in thin film form developed in the laboratory to obtain MoS_2 films. We compare the properties of the films obtained with and without an Ni interfacial layer. The properties of the films obtained in an open and in a closed reactor are also compared.

2. Experimental procedure

2.1. Synthesis of the film

For economic reasons mica sheet substrates have been used. They were systematically cleaved before their introduction into the deposition chamber. First, a thin (10–20 nm) NiCr (20 at % Cr) layer was deposited on the mica substrate. The NiCr alloy was provided by Goodfellow. Thicker films have been deposited in order to check the composition of the deposit by electron microprobe. It was shown that the composition of the NiCr film was the same as that of the starting material in the precision range of the apparatus.

Then, the thin Mo and S layers were sequentially deposited in vacuum. S was evaporated by classical thermal evaporation, Mo was evaporated by an electron beam. The MoS_2 films were synthesized by solid state reaction from thin Mo and S layers. The evaporation rates and film thicknesses were measured *in situ* by the vibrating quartz method. The number of layers varied from four to eight in order to deposit

0022–2461

Mo/S/Mo, ... , Mo/S structures. The last sulphur layer was used to protect the last Mo layer from oxidation during transfer from the deposition apparatus to the oven for the post annealing treatment. The thickness of the last sulphur layer was about 100 nm and the thicknesses of the other layers were calculated to achieve the desired composition, varying from 8 to 25 nm and from 60 to 150 nm for Mo and S, respectively, while the evaporation rate was 1 and 10 nm s^{-1} for Mo and S, respectively.

The technique was roughly the same as previously described [6]; however the thickness of the Mo and S layers were calculated in order to achieve the atomic ratio Mo:S = 1:3 and not 1:2 as previously.

We have used two methods for the post annealing treatment. The first one is called a "closed reactor" and is similar to the one used earlier: the sample is sealed under vacuum in a silica tube. The second one is called an "open reactor". In that case the sample is introduced in a silica tube placed in an oven. Before annealing, the whole silica tube is put under vacuum and the sample is heated at 375 K for 30 min. Then an argon flow is introduced into the silica tube (40 l h^{-1}) and the sample is heated up to 1073 K for 30 min. Finally, the sample is cooled down.

In the case of the closed reactor, because there is an upper sulphide layer, during the annealing this layer provides a sulphur atmosphere and at the end of the process, during the cooling of the tube, there is some sulphur condensation at the surface of the film. Therefore these films have to be annealed under dynamic vacuum in order to sublimate this surface excess of sulphur, which is not necessary for the films obtained in an open reactor.

2.2. Thin film characterization

The structure of the films was examined using an analytical X-ray system type Diffract AT V3.1 Siemens instrument that used an EVA graphics program. The wavelength, λ, was 0.154 06 nm.

The surface topography was observed with a field effect scanning electron microscope Jeol F 6400. Electronic microanalyses were performed using a Jeol 5800 LV scanning electron microscope equipped with a PGT X-ray microanalysis system, in which X-rays were detected by a germanium crystal. XPS measurements were performed with a magnesium X-ray source (1253 eV) operating at 10 kV and 10 mA. Data acquisition treatment was realized using a computer and a standard program. The quantitative studies were based on the determination of the Mo3*d* and S2*p* peak areas with 2.5 and 0.125, respectively, as sensitivity factors. The sensitivity factors of the spectrometer were given by Leybold, the manufacturer.

Since a thin interfacial Ni layer was used to achieve well crystallized films, we have studied the Ni distribution all over the thicknesses of the MoS_2 films. The depth profile was studied by recording successive XPS spectra of Ni2*p*, Mo3*d* and S2*p* obtained after ion etching for short periods. Using an ion gun, sputtering was accomplished at pressures of less than 5×10^{-4} Pa with a 10 mA emission current and 5 kV beam energy. For quantitative depth profile analysis the $Ni2p_{3/2}$ sensitivity factor used was 4.5.

At the surface of the film there is a carbon–carbon bond corresponding to surface contamination. In the apparatus used the C–C band has a well defined position at 284.6 eV and the carbon peak was used as a reference to estimate the electrical charge effect.

The majority carrier type was studied by the hot probe technique. The conductivity of the MoS_2 film was measured in the temperature range from 100 to 500 K on planar samples. Evaporated gold electrodes were used, because it has been shown that gold gives good ohmic contacts [6]. Conductivity measurements were carried out in the dark using an electrometer (Keithley 617).

Photoconductivity measurements were performed with a lock in amplifier. (Photoconductivity measurements have been carried out at the LEMM in Bordeaux I). The chopper frequency was 20 Hz, a $\frac{1}{4}$ monochromator and a quartz halogen lamp provided the incident radiation (210 W). The applied voltage during measurements was 10 V.

3. Results and discussion

First of all we compare the properties of the films obtained in an open reactor to those of the films obtained in a closed reactor. Then we compare the properties of the films obtained in the same conditions, on a bare mica sheet and on an NiCr–mica sheet.

3.1. Films obtained in a closed reactor and in an open reactor: a comparison

These films were characterized by X-ray diffraction (XRD) and SEM studies. For this first study, very thin films (thickness $\approx$50 nm) were used, which means that only two sulphur and two molybdenum layers were deposited. The thicknesses of the molybdenum layers were 8 nm, which means that these layers were probably discontinuous, which can explain that, mainly in the case of the open reactor, the films were discontinuous. The annealing conditions used were 1073 K for 30 min. We can see in Fig. 1 that in an open reactor

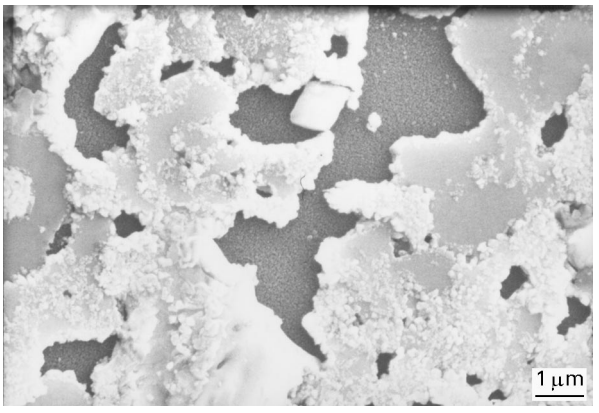

Figure 1 Microphotograph of a thin MoS_2 film (50 nm) obtained with an open reactor.

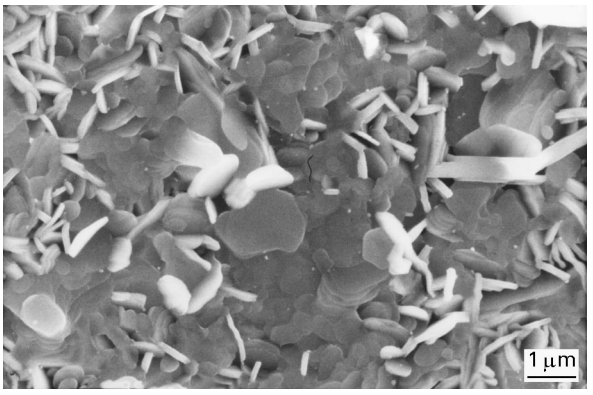

Figure 2 Microphotograph of a thin MoS_2 film (50 nm) obtained with a closed reactor.

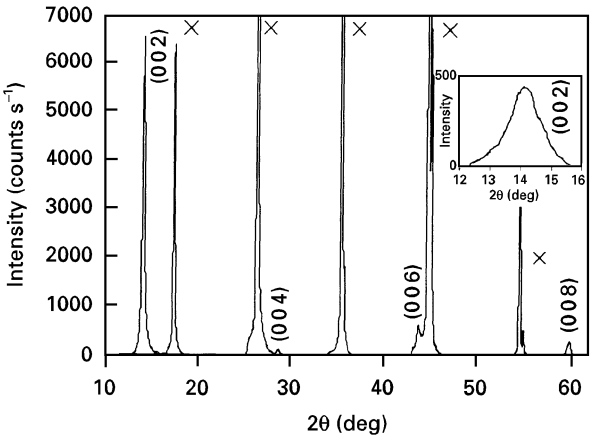

Figure 3 XRD spectrum of a MoS_2 (NiCr–mica) film, 150 nm thick, annealed at 1073 K for 30 min (X) mica substrate peaks. Inset: (0 0.2) peak of a MoS_2 (mica) film (150 nm thick).

the films are discontinuous, but large grain sizes are achieved.

These results obtained with this open reactor have been compared with those obtained with the same films annealed in a closed system. If these films appear to be more continuous, it can be seen after annealing (Fig. 2) that the texture of the films is poor and that the grain size is smaller than that obtained with the open reactor. Moreover, the intensity and the full-width-at-half-maximum (FWHM) of the (0 0.2) XRD diffraction peaks (not shown) are higher for the intensity and smaller for the FWHM in the case of the films obtained in an open reactor, which demonstrates their higher crystalline quality. Another advantage of the open reactor is economical, because the same reactor can be used many times. Therefore, this new technique has been used to obtain thicker MoS_2 films (150 nm). A greater film thickness was used in order to avoid the high density of pinholes present in the very thin films.

3.2. Films obtained with and without a thin interfacial NiCr layer: a comparison

Here we compare the properties of the films obtained by using an NiCr coated mica sheet, which is called "MoS_2 (NiCr–mica)", and those of the films obtained directly on a mica sheet which is called "MoS_2 (mica)". Even, if there is some overlap of MoS_2 and mica peaks (0 0.6, 0 0.8), it can be seen in Fig. 3 that the MoS_2 (NiCr–mica) films are not only crystallized in the 2H–MoS_2 structure, but that the (0 0.2) peak intensity is far higher than that (inset Fig. 3) obtained with MoS_2 (mica) films of the same thicknesses (150 nm) and annealed in the same conditions. Moreover the FWHM of the (0 0.2) peak is far smaller. The thickness of the crystallites was estimated from the FWHM of the (0 0.2) peak. In the case of MoS_2 (NiCr–mica) films, the FWHM of the (0 0.2) X-ray diffraction peak is of the same order of magnitude as that obtained with a reference powder. Therefore it can be concluded that the grain size is at least 100 nm or more, which means that it is of the same order of magnitude as the thickness of the film. In the case of MoS_2 (mica) films the grain size, deduced from the FWHM, is about 10 nm, which is far smaller than the film thickness.

We have seen from Fig. 1 that, along the surface plane, the grain size is of the order of 0.5 μm. For thicker films the grains are not so well resolved because the films are continuous without pinholes (Fig. 4a). Moreover, some geometrical features (straight lines) are visible. These features appear to correspond coarsely to geometrical defaults of the cleaved mica substrate. The MoS_2 (mica) films appear strongly inhomogeneous with large crystallites (0.1–0.2 μm) randomly spread in a polycrystalline matrix (Fig. 4c). The crystallites of this matrix appear to be very small. At higher magnification, the surface of the MoS_2 (NiCr–mica) film appears quite smooth with small "reliefs" randomly spread (Fig. 4b). The electron microprobe quantitative analyses show that all the films are stoichiometric. They also show that some nickel can be found in MoS_2 (NiCr–mica) films. However, there is no correlation with the intensity of the nickel peak and the density of "reliefs" in the analysed domains. Therefore no correlation can be established between the "reliefs" and the nickel. It should be noted that the films are quite thin for the microprobe technique, which induces large uncertainties in the measurements. If we were unable to study the repartition of Ni along the plane surfaces of the film; it has been studied by XPS through the depth of the film.

First we studied the surface of the films. The XPS spectra are reported in Fig. 5. It can be seen that the binding energies of the peaks are in good agreement with the values expected in the case of MoS_2. Decomposition of the signals demonstrates that the peaks correspond to only one signal, which means that neither an oxide nor a free element are present in these films. The quantitative analysis shows that the films are stoichiometric. The nickel present at the film–substrate interface before annealing can be detected at the surface of the film (0.25%). Its atomic percentage appears to increase when the etching time increases. It is well known that the sputtering efficiency of sulphur is far higher than that of molybdenum

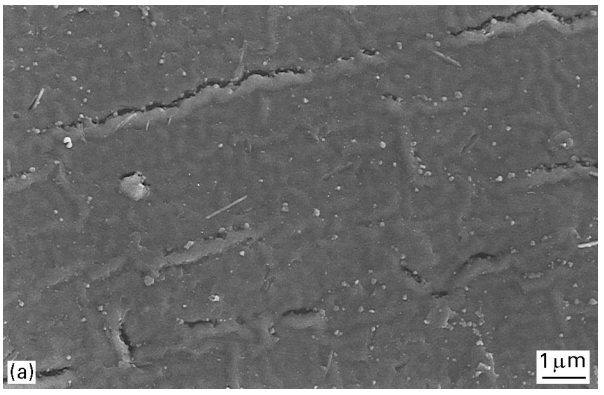

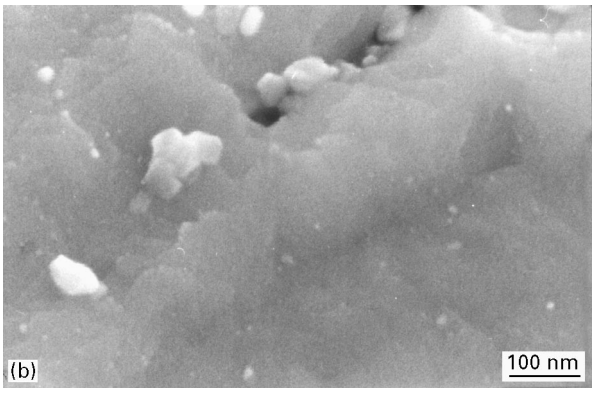

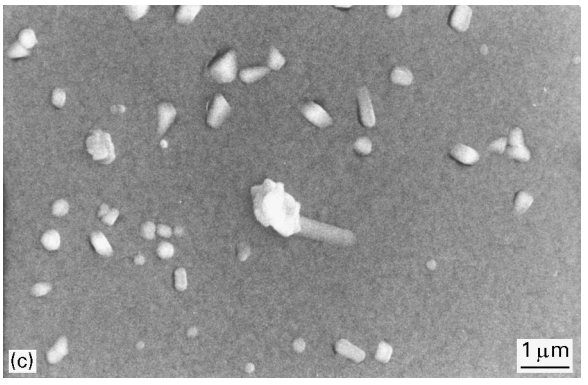

Figure 4 Microphotograph of 150 nm thick films annealed at 1073 K for 30 min: (a) MoS_2 (NicCr–mica) film (b) MoS_2 (NiCr–mica) film at higher magnification, and (c) MoS_2 (mica) film.

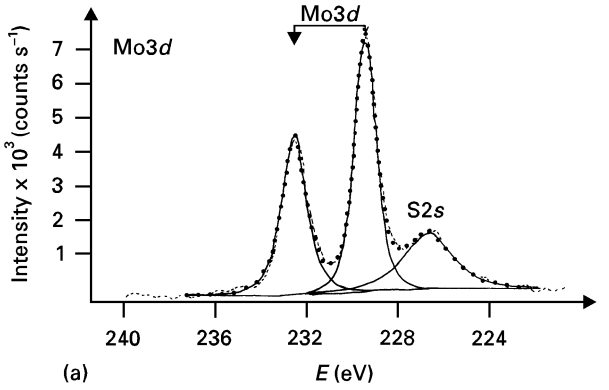

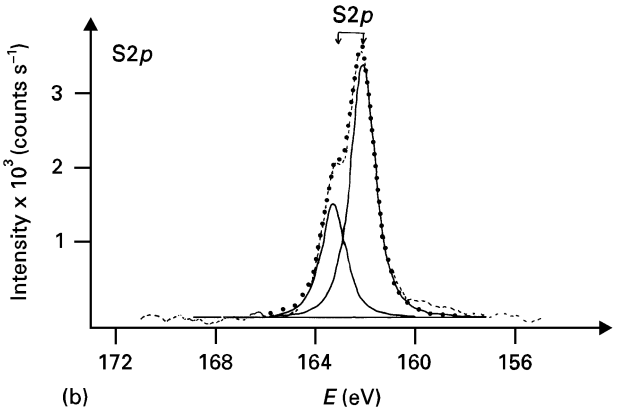

Figure 5 XPS spectra of (a) Mo3*d* and (b) S2*p* peaks: (– – –) experimental curve, (●●●) theoretical curve, and (——) components of the corresponding doublet.

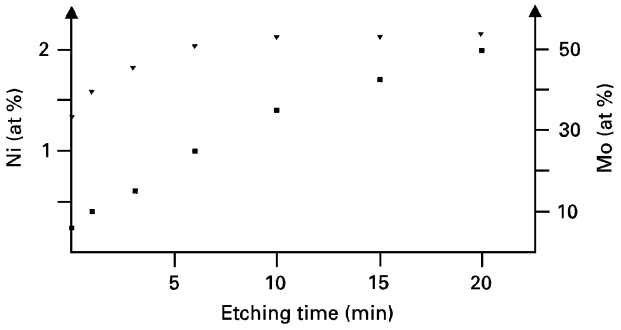

Figure 6 XPS depth profiling of a MoS_2 (NiCr–mica) film. (■) at % Ni, (▼) at % Mo.

and also of nickel. Therefore in the case of MoS_2, after etching, there is a molybdenum excess. Depth profiling of MoS_2 is reported in Fig. 6. It can be seen that the atomic concentration of molybdenum stabilizes after 10 min etching. This is not the case for nickel. Therefore there is probably an increase of the nickel concentration all over the depth of the film. After etching for 10 min there is about 1 at % nickel in the film and 2 at % after etching for 20 min (Fig. 6). Therefore it appears that, during annealing, nickel diffuses along the thickness of the film and there is a concentration gradient from the bottom of the film.

It has been shown, by the hot probe technique, that the films were p-type and the gold electrodes gave good ohmic contacts. The conductivities of the films have been measured between 100 and 500 K. At higher temperatures there were some difficulties in obtaining a good adherence of the electrical contact on the mica sheet. In Fig. 7, the results obtained with MoS_2 (NiCr–mica) films can be compared with those obtained with the MoS_2 (mica) films grown without Ni. It can be seen that, at room temperature, the conductivity, which is at least multiplied by a factor of ten ($0.1\ \Omega^{-1}\ cm^{-1} < \sigma < 0.25\ \Omega^{-1}\ cm^{-1}$), is nearly of the same order as that of single crystals [10]. Moreover, it has been shown, by using a model of potential fluctuations at the grain boundaries [11], that the conductivities of the films obtained without Ni were controlled by inhomogeneous grain boundaries, because the plot of $\ln\sigma$ versus $(10^3/T)$ did not follow an Arrhenius law but was better fitted by a parabola. In the case of MoS_2 (Ni–mica) films it appears that the

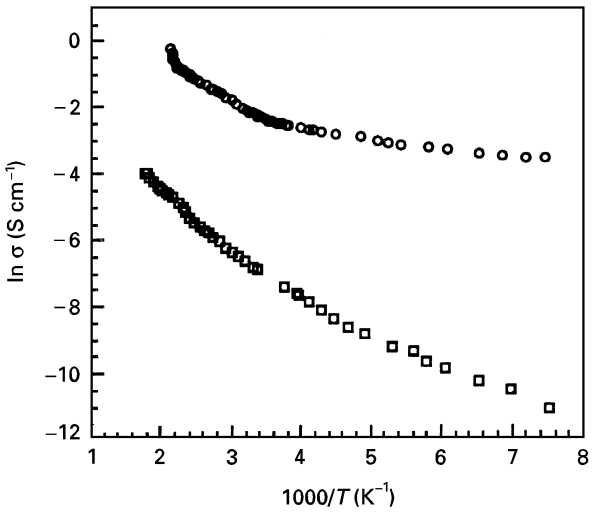

Figure 7 Temperature dependence of the electrical conductivities of MoS_2 (NiCr–mica) (○) and MoS_2 (mica) (□) films.

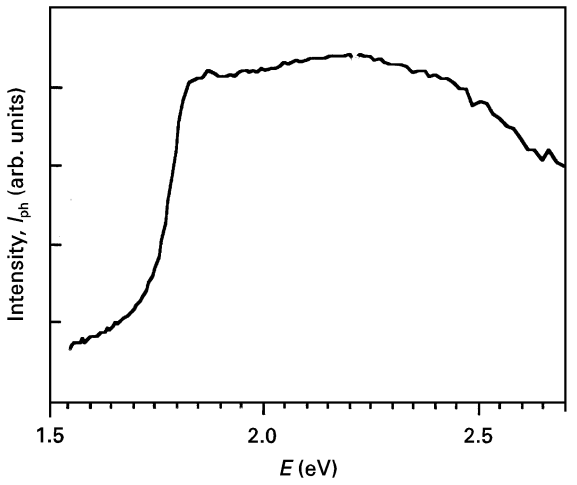

Figure 8 Photocurrent spectrum of an MoS_2 (NiCr–mica) film.

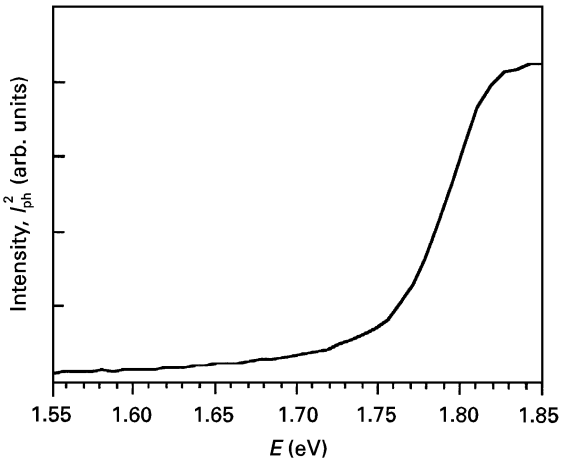

Figure 9 Square of the photocurrent versus light energy.

curve $\ln\sigma$ versus $(10^3/T)$ does not systematically follow a parabola law [6] but sometimes some activation energies can be deduced from linear domains above room temperature. Therefore, in that case, more classical grain boundary theories can be used [12, 13]. These grain boundary trapping theories assume that the grain boundaries are highly disordered resistive domains with trapping states, which capture free carriers and therefore make them immobile. These charged states at the grain boundaries create depleted regions and potential barriers that hinder the passage of carriers from a grain to the neighbouring ones. Therefore, for the polycrystalline trapping model, the resistance, R, is given by [13]

$$R = (R_1 + R_2) \rightarrow \rho = \rho_1\left(1 - \frac{2W}{L}\right) + \rho_2\left(\frac{2W}{L}\right)$$

where W is the width of the depleted region, L is the grain length, and subscript 1 is related to the grain, and subscript 2 to the boundary.

In the case of the MoS_2 (Ni–mica) film the room temperature conductivity is not very different from that of a MoS_2 single crystal. Therefore, ρ_2 should be of the same order as ρ_1 and should be taken into account. It is well known that, over the high temperature range, the conductivity is often no longer limited by the grain boundaries but rather by the conductivity of the grains. Over this temperature range, the energy of the free carriers is high enough to activate them beyond the barriers and the electrons are excited in the extended states of the conduction band. Therefore, theoretically, the thermal energy gap, ΔE, can be estimated from the slopes. The difficulty of keeping the electrical contact at high temperature, prevents us from seeing this domain clearly. However, we can see a strong increase of ΔE ($\Delta E \approx 1.1$–1.2 eV) at temperatures higher than 450 K, which means that we are probably just at the beginning of the intrinsic domain.

In the case of the curve for a MoS_2 (NiCr–mica) film, Fig. 7, in the middle temperature range (300–450 K) the evolution of conductivity with reciprocal temperature follows nearly an Arrhenius law with an activation energy of about 115 meV, which shows that the conductivity is merely controlled by grain boundaries. In that case we have [12]

$$\sigma T^{1/2} = \sigma_0 \exp\left(-\frac{q\Phi_B}{kT}\right)$$

Φ_B being the barrier height at the grain boundary K the Boltzman constant and q the electronic charge.

Therefore in the case of these MoS_2 (NiCr–mica) samples, $\Phi_B \approx 115$ meV which is smaller than the value obtained in the case of the MoS_2 (mica) samples where $\Phi_B \geqslant 150$ meV [6].

The current under illumination has been measured at room temperature in the range 400–800 nm. While there was not any photocurrent measurable in the experimental conditions used, in the case of the MoS_2 (mica) samples, the MoS_2 (NiCr–mica) films were photosensitive. Fig. 8 shows a typical photocurrent spectrum of a polycrystalline MoS_2 (NiCr–mica) film. As can be seen the quantum efficiency begins to increase strongly at an energy of about 1.7–1.8 eV. An analysis of the rising portion of the curve in Fig. 9 (i.e. a plot of the square of the photocurrent versus light

energy) yields a straight line from which a direct band gap energy of 1.7 eV can be extracted. This is in good agreement with the reported direct band gap energy, Eg_{di} of 1.65 eV for single crystal MoS_2 [14]. If, on the other hand, the data obtained before the strong increase of the photocurrent are plotted as the square root of the photocurrent versus light energy a straight line can be extrapolated and in this case the band gap energy is 1.29 eV. This is not very different from the indirect band gap energy, Eg_{ind}, of this material [14]. It shows that, even in the small absorption domain ($Eg_{ind} < h\nu < Eg_{di}$), the films are photosensitive, which confirms their good quality.

4. Conclusions

We have shown that annealing of a starting material (thin layers of Mo and S sequentially deposited) containing an excess of sulphur (MoS_3) permits us to obtain MoS_2 films. The films obtained in an open reactor under an argon flux are better than those obtained in a closed reactor in a sulphur atmosphere. The crystallinities and the textures of the former films are better.

A systematic comparison of the properties of the films, obtained on NiCr coated mica substrates and on bare mica substrates, has shown that an NiCr layer is necessary to obtain high quality MoS_2 films. After annealing at 1070 K for 30 min in an open reactor these films are textured with the *c*-axes of crystallites perpendicular to the plane of the substrate. The thicknesses of the crystallites are similar to those of the films (150 nm). The films are homogeneous and their conductivities are of the same order as that of single crystals. The films are photoconductive, which is very promising for photovoltaic applications.

The films obtained at the same time in the same conditions, but on a bare mica sheet, have very different properties. They are badly crystallized, their grain sizes are smaller than the thicknesses of the films, their conductivities are far smaller than that of a single crystal and they are not photoconductive.

Therefore, probably as proposed by Salitra *et al.* [15] it is necessary that a melting Ni–S_x phase forms. Such a liquid phase induces better crystallization by increasing the mobility of the constituents at the grain boundaries.

Acknowledgements

The authors wish to thank Mrs Barreau and Le Ny for performing scanning electron microscope and microprobe studies, Mr. Lignier for photoconductive measurements. This work was supported by a contract between the EEC and the LPME (JOU II CT 93 0352) and a contract between France and Algeria (CMEP DPU).

References

1. H. TRIBUSCH, *Solar Energy Mater.* **1** (1979) 257.
2. G. KLINE, K. K. KAM, R. ZIEGLER and B. A. PARKINSON, *ibid.* **6** (1982) 337.
3. R. TENNE and A. WOLD, *Appl. Phys. Lett.* **47** (1985) 707.
4. G. PRASAD and O. W. SRIVASTAVA, *J. Phys. D* **21** (1988) 1028.
5. A. SEGURO, M. C. MARTINEZ TOMAS, B. MORI, A. CASANOVAS and A. CHEVY, *Appl. Phys. A* **44** (1987) 1249.
6. J. POUZET, H. HADOUDA, J. C. BERNEDE and R. LE NY, *J. Phys. Chem. Sol.* **57** (1996) 1363.
7. A. JAGER-WALDAU, M. C. LUX-STEINER, G. JAGER-WALDAU and E. BUCHER, *Appl. Surf. Sci.* **70/71** (1993) 731.
8. A. ENNAOUI, S. FIECHTER, K. ELLMER, R. SCHEER and K. DIESNER, *Thin Solid Films* **261** (1995) 124.
9. C. BALLIF, M. REGULA, P. E. SCHMID, M. REMSKAR, D. SANJINES and F. LEVY, *Appl. Phys. A* **62** (1996) 543.
10. K. K. KAM and B. A. PARKINSON, *J. Phys. Chem.* **86** (1982) 463.
11. J. H. WERNER, *Solid State Phenomena* **37/38** (1994) 213.
12. J. W. SETO, *J. Appl. Phys.* **49** (1984) 5365.
13. A. OUADAH, J. C. BERNEDE, J. POUZET and M. MORSLI, *Phys. Status Solidi* **134** (1992) 455.
14. E. BUCHER, in "Photoelectrochemistry and photovoltaics of layered semiconductors", edited by A. Aruchamy (Kluver Academic, Dordrecht, NL, 1992) p. 1.
15. G. SALITRA, G. HODES, E. KLEIN and R. TENNE, *Thin Solid Films* **245** (1994) 180.

Received 24 June 1996
and accepted 10 February 1997